# DEVELOPMENT AND ANALYSIS OF A LOW POWER A-C INSTRUMENT SERVOMECHANISM



by

JOHN IRVIN GARRETT

B. S., Kansas State University, 1960

---

A MASTER'S THESIS

submitted in partial fulfillment of the

requirements for the degree

MASTER OF SCIENCE

Department of Electrical Engineering

KANSAS STATE UNIVERSITY
Manhattan, Kansas

1964

Approved by:

Charles H. Warnick
Major Professor

TABLE OF CONTENTS

INTRODUCTION..... 1

FIXED PHASE SWITCH DEVELOPMENT..... 4

Switching Circuit Using Shockley Diode Characteristics.....13

Servo System Using Fixed Phase Switch.....19

AMPLIFIER DEVELOPMENT.....21

OTHER ELEMENTS OF THE SYSTEM.....26

The Servo Motor.....26

The Rate Generator.....26

The Error Detector.....26

The Gear Train.....28

The System Load.....28

LINEARIZING THE MOTOR CHARACTERISTICS.....28

DETERMINATION OF SYSTEM CONSTANTS.....30

AMPLIFIER CHARACTERISTICS.....31

Describing Function of the Amplifier.....32

SYSTEM ANALYSIS.....33

System No. 1.....36

System No. 2.....40

System No. 3.....48

System No. 4.....50

SIMULATION AND RESULTS.....50

Amplifier Simulation.....51

Backlash Simulation.....51

Rate Generator Drive Excitation.....51

Results.....60

CONCLUSIONS.....60

ACKNOWLEDGMENTS.....62

REFERENCES.....63

# INTRODUCTION

The use of servomechanisms to operate displays on aircraft instruments is by no means new. Servo systems have been used for many years to display gyro and compass information to the pilot. Such control systems are commonly called instrument servos. Essentially all of these systems are carrier frequency servos utilizing the basic carrier frequency of 400 cycles per second. The servo motor used almost exclusively in modern aircraft instruments is a size 8, two-phase induction servo motor which measures 0.750 inch in diameter. There are several important reasons why such motors are used, among which are light weight, no commutator, and small physical size. Amplifiers to drive the induction servo motor are also somewhat easier to construct than would be their equivalent d-c counterparts.

Various lengths of servo motors and motor-generators have been available over the years, although the trend in recent years has been toward shorter motors and motor-generators. The maximum output torque available has been held essentially constant, but with new advances with respect to construction techniques, manufacturing tolerances, and motor design, the case length of the size 8 motor-generator has been reduced to 1.25 inches. These units require 3 watts of fixed phase motor power and 2 watts of fixed phase generator power. The fixed phase power has not been reduced despite the reduction in size.

Until recently, the number of servo motor-generators in the average

instrument was three of less. Thermal problems were anticipated in these units, however, the temperature rise was not great enough to merit a heat reduction investigation.

Early in 1962, a completely new type of flight director instrument was proposed and development initiated. This instrument (Fig. 1) brought together for the first time, gyro and command information showing the aircraft in simulated flight. A minature runway was also incorporated showing altitude and localizer deviation for aids in landing the aircraft. Each channel was driven by a servomechanism. This requirement doubled the number of servo motor-generators required by previous systems.

With six servo motors now necessary there was certain danger of overheating the instrument unless definite steps were taken to reduce the operating power of the instrument. If no compensations were made, there could be as much as 40 watts consumed by the instrument under normal conditions. Seventy-five per cent of the total power would be consumed by the fixed phases of the motor-generators. The remainder of the power would be consumed in lighting, synchros, and other minor power consuming elements.

A logical approach to lowering the heat dissipation of the instrument was to study the possibility of lowering or eliminating the fixed phase power of the servo motor-generators when at null.

A second requirement was also necessary although it was not immediately apparent. The increased number of servo motors required was generated because additional types of displays were desired in the instrument. These displays, out of necessity of easy viewing, were placed at the front of the instrument. This created gearing and mechanical design problems.


Fig. 1 Flight Director Instrument

The steps necessary to solve the display proximity problems resulted in a system with more gearing friction than had ever been experienced in previous instruments. To provide the same accuracy of positioning as was required in early models of similar instruments it was necessary to incorporate a higher gain amplifier.

It was desired to maintain the speed of response of earlier models and the gear trains were designed to have approximately the same length, i.e., turns ratio. This meant that with increased torque required, the maximum output power of the servo amplifier would necessarily have to be increased. This was possible because the amplifiers previously used did not provide output power near the maximum that the motor was capable of consuming. Thus it was realized that an amplifier with three new requirements would have to be developed.

1. Circuitry to control the fixed phase.
2. Amplifier gain greatly in excess of existing amplifiers.
3. A dynamic range greater than that of existing amplifiers.

It will be the purpose of this thesis to describe and analyze the systems that resulted as an outgrowth of the stated requirements.

## FIXED PHASE SWITCH DEVELOPMENT

One solution to the problem of controlling the fixed phase of the servo motor was to use a switch which would be controlled by some function of the system error. A question which immediately presents itself when considering the switch approach is that of whether the fixed phase of the generator can also be controlled as a function of system error.

The first step in the design of a solid state switch for controlling the fixed phases of the motor-generator was to examine the various circuits and devices that were available. There seemed to be only three types of circuits available. Figure 2 shows circuits using two transistors. Figure 3 shows a basic bridge arrangement in conjunction with one transistor and Fig. 4 shows a transistor, diode, capacitor arrangement. In all cases, except that of Fig. 2b, silicon controlled rectifiers (SCR's) can be used in place of transistors. In Fig. 2a and 3, a floating supply would be necessary to drive the switch "ON". Therefore attention was directed to the circuit of Fig. 4 with an SCR in place of the transistor, where a transformer was not needed to supply a floating drive. A large capacitor was necessary, however, to give proper operation. This will be apparent after further comments of the theory of operation of the amplifier.

It was now necessary to develop a circuit to drive the gate of the SCR. A two-state device ("ON" or "OFF") was desired, therefore, attention was directed toward circuits having two output levels. The Schmidt trigger seemed to have characteristics that could be developed for this application.

The circuit investigated is shown in Fig. 5. In this circuit $R_1$ is of low enough value that $Q_2$ is "ON". In this condition, the output voltage is given by the following expression.

$$V = \frac{E\ R_3}{R_2 + R_3} \qquad (1)$$

This is, of course, the case when $V_1 < V_2$. Now let $V_1$ be raised to a potential above $V_2$. $Q_1$ begins to draw current and $Q_2$ ceases to draw

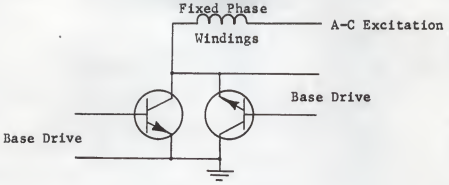


(a)

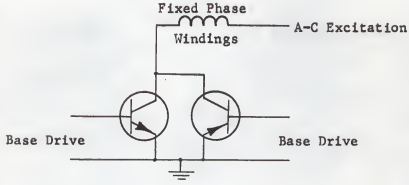


(b)

Fig. 2 Two transistor A-C switches

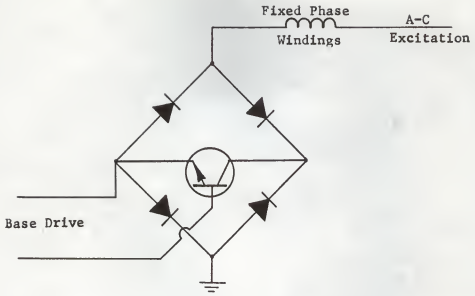


Fig. 3 Bridge A-C switch

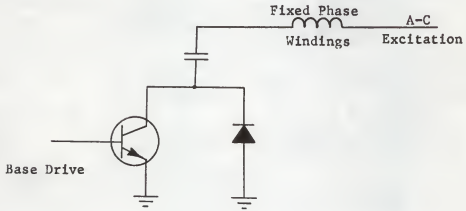


Fig. 4 Transistor, diode, capacitor A-C switch

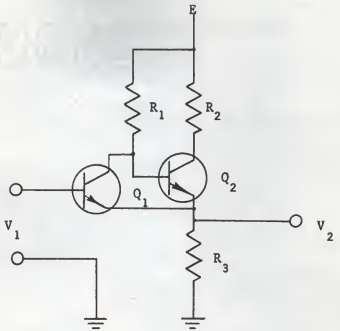


Fig. 5 Schmidt trigger switching circuit

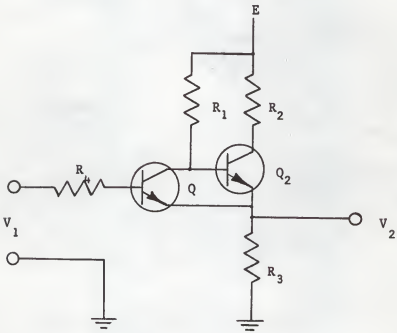


Fig. 6 Modified Schmidt trigger circuit

current. $V_2$ will, however, follow $V_1$, since $V_1$ is above the original $V_2$ and the diode current of the base circuit of $Q_1$ is forward biased.

If an additional resistor is placed in the circuit to give Fig. 6, the response will be quite different. When $V_1 < V_2$ then $Q_2$ is "ON" and $Q_1$ is "OFF". As $V_1$ is increased to a potential just above $V_2$, $Q_1$ begins to draw base current and $Q_2$ turns "OFF". Now the voltage at the base of $Q_1$ can drop as the base potential of $Q_2$ drops. This circuit then gives two distinct levels of output voltage. Another stage is necessary to get the proper drive on the SCR, because the phase of the output voltage is opposite of that required. The resulting complete circuit is illustrated in Fig. 7. The breakdown voltage of the Zener diode is above the low voltage state of $Q_2$ but below the high voltage state. Equations for determining the component values in the circuit are given in the following paragraph.

$R_6$ is determined by the D-C supply voltage and the gate current $I_g$ necessary to switch the SCR. $I_g$ of a typical SCR that is applicable for this switching function is specified at 10 milliamperes.

$$R_6 = \frac{E}{10 \text{ ma.}} \tag{2}$$

$R_7$ is determined by the SCR specifications and is 1000 ohms. Since 10 milliamperes will exist in $Q_3$ when it is "ON" the base current to switch $Q_3$ "ON" must be at least

$$I_{b_3} = \frac{10 \text{ ma.}}{\beta_3} \tag{3}$$

where $\beta_3$ is the current gain of $Q_3$. Typical modern transistors have a $\beta$

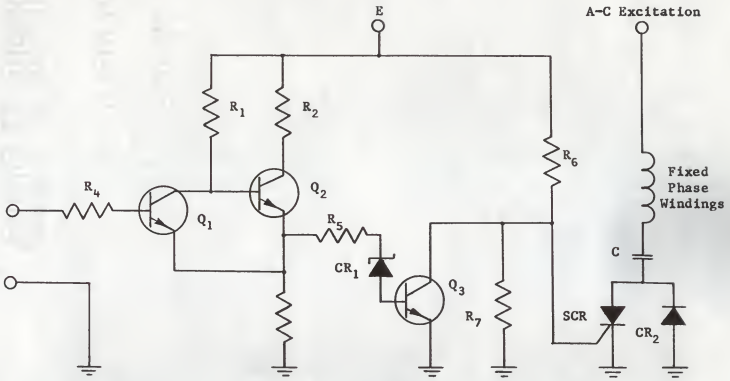


Fig. 7 Complete fixed phase switching circuit

of 40 or more. In order to be sure that $Q_3$ is "ON" a $\beta_3$ of 20 will be assumed; therefore

$$I_{b_3} = \frac{10 \text{ ma.}}{20} \tag{4}$$

The design voltage at which the SCR should switch and also the voltage at which the circuit will return to its original state were necessary at this point in the circuit design. The excitation voltage at which the circuit switches to its low voltage output state should be determined by the servo amplifier output at maximum allowable system static error. Since the output of the servo amplifier is a-c, rectification is necessary before it can be applied as excitation voltage to the drive circuit. The value of excitation voltage to make the circuit switch to its low voltage output state is linked to the circuit parameters by Eq. 1.

The value of excitation voltage to make this circuit return to its original state (high output voltage) should be considerably above the noise level output of the amplifier at null. This guarantees that the circuit will always turn "OFF" at null. This voltage is linked to the circuit parameters by the following equation.

$$V = \frac{E\ R_3}{R_1 + R_3} \tag{5}$$

The Zener diode in the base feed of $Q_3$ was inserted to completely remove the base current of $Q_3$ when the emitter of $Q_2$ is at the voltage given by Eq. 5. The voltage of Eq. 1 was taken to be 20 volts and V of Eq. 5 to be 6 volts. By using a 10 volt Zener diode, the value of $R_5$ was determined by the following equation.

$$R_5 = \frac{E_1 - V_z}{I_g(1/\beta_3)} = \frac{20 - 10}{I_g(1/20)} = \frac{200}{I_g} \tag{6}$$

where $V_z$ is the reverse breakdown of the Zener diode. The collector current of $Q_2$ was selected to be

$$I_{c_2} = 10\ I_{b_3} \tag{7}$$

so that the Schmidt trigger would not be significantly loaded. Then

$$I_{c_2} = \frac{E}{R_2 + R_3} \tag{8}$$

and when $Q_2$ is "ON", the emitter of $Q_2$ should be at 20 volts which is the design voltage. Therefore

$$R_3 = \frac{20 \text{ volts}}{I_{c_2}} \tag{9}$$

and

$$R_2 = \frac{E - I_{c_2} R_3}{I_{c_2}} = \frac{E}{I_{c_2}} - R_3 \tag{10}$$

Finally

$$I_{c_1} = \frac{6 \text{ volts}}{R_3} \tag{11}$$

and

$$R_1 = \frac{E}{I_{c_1}} - R_3 \tag{12}$$

These equations will suffice if the base current of $Q_2$ is less than one tenth of the collector current of $Q_2$. If this is not the case then the loading effects of $Q_3$ should be entered into Eq. 8.

Final adjustments on the length of time that the circuit will stay "ON" after the input has dropped to zero can be made by adjusting C and R of the input circuit.

## Switching Circuit Using Shockley Diode Characteristics

The Shockley diode has characteristics that are particularly attractive for switch applications since it is always in the "ON" or "OFF" state. The manner in which the two states are obtained makes the diode applicable for the specific purpose. The diode is "OFF" or non-conducting until the voltage across the diode reaches breakdown potential ($V_{BD}$). At this voltage the diode turns "ON" or to the conducting state and remains there until the current falls to dropout current ($I_{DO}$).

The switching circuit is shown in Fig. 8 where the Shockley diode is $CR_2$. To analyze this circuit consider the gate of the SCR to be at ground potential and the Shockley diode to be a switch with specific characteristics. These characteristics are that the switch will turn "ON" when 20 volts is applied across it and will continue to stay on until less than 10 milliamperes of current flows through it. A further assumption will be that once the Shockley diode has turned "ON" no more charge will be deposited on $C_1$ from the amplifier. The circuit to analyze is then that of Fig. 9.

When $S_1$ closes, the base current of $Q_1$ will have the form

$$i_b = \frac{20}{R_1 + \beta R_2} \exp\left(-\frac{t}{C_1(R_1 + \beta R_2)}\right) \qquad (13)$$

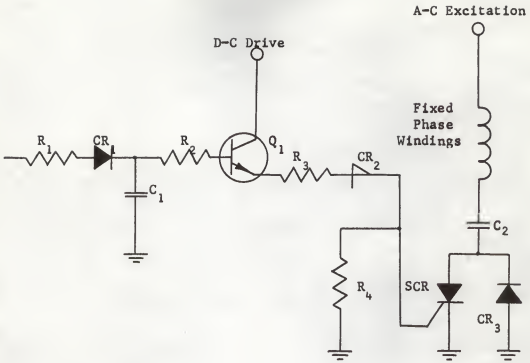


Fig. 8 Fixed phase switching circuit using Shockley diode

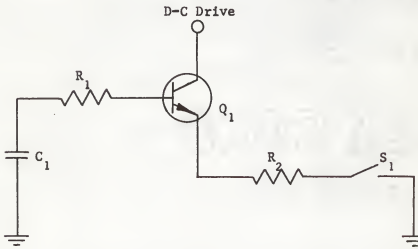


Fig. 9 Equivalent Shockley diode circuit for analysis

Equation 13 will hold until

$$i_b = \frac{10 \text{ ma.}}{\beta_1} \tag{14}$$

When the condition of Eq. 14 is reached, $S_1$ will open and there will no longer be any base current of collector current in $Q_1$. Since $S_1$ is open there will be no gate current in the SCR and it will, therefore, be open. The length of time that the Shockley diode will be conducting is found by substituting Eq. 14 in Eq. 13 to get

$$\frac{10 \text{ ma.} \ (R_1 + \beta R_2)}{20 \ \beta_1} = \exp\left( - \frac{t}{C_1(R_1 + \beta R_2)} \right) \tag{15}$$

from which

$$t = - C_1(R_1 + \beta R_2) \ln\left( \frac{10 \text{ ma.} \ (R_1 + \beta R_2)}{20 \ \beta} \right) \tag{16}$$

There is an upper limit on $R_1 + \beta_1 R_2$ which is given by

$$R_1 + \beta R_2 = \frac{20}{10 \text{ ma.}} \tag{17}$$

Equation 17 gives the combination of $R_1$, $R_2$, and $\beta_1$ to just produce 10 milliamperes of current through the Shockley diode when 20 volts of charge exists on $C_1$. The voltage on $C_1$ necessary to give a Shockley diode current of 10 milliamperes is given by Eq. 18.

$$V_{C_1} = \frac{10 \text{ ma.}}{\beta_1} R_1 + R_2 \times 10 \text{ ma.} \tag{18}$$

$R_1$ was reduced to zero so that

$$t = - C_1 \ \beta \ R_2 \ln\left( \frac{10 \text{ ma.} \times R_2}{20} \right) \tag{19}$$

This eliminated one resistor in the circuit and also simplified the equations. By examining Eq. 19 it can easily be recognized that in order to make $t > 0$:

$$\frac{10 \text{ ma.} \times R_2}{20} < 1 \tag{20}$$

or

$$R < 2000 \text{ ohms} \tag{21}$$

The length of time that the circuit will be "ON" is controlled by varying $R_2$ and/or $C_1$. The length of time that the switch will be "ON" is shown in Fig. 10 for various values of $C_1\beta$. A certain value of $R_2$ will hold the SCR "ON" for a maximum length of time and can be found by setting $(\partial t)/(\partial R_2) = 0$. By performing the indicated operation on Eq. 19, the result is

$$\frac{\partial t}{\partial R_2} = - C_1 \beta \{ 1 + \ln( \frac{10 \text{ ma.} \times R_2}{20} ) \} \tag{22}$$

This gives

$$R_2 = \frac{20}{10 \text{ ma.}} e^{-1} \tag{23}$$

The Shockley diode circuit works quite well; however, the length of time that the SCR is "ON" depends directly upon the $\beta$ of the transistor. The circuit therefore behaves differently for each transistor used. By using an additional transistor the circuit can be modified to be almost completely independent of the transistor parameters. The revised circuit is shown in Fig. 11. The impedance looking into the base of $Q_1$ when the Shockley diode is shorted is the product of $\beta_1$, $\beta_2$, and $R_3$. If

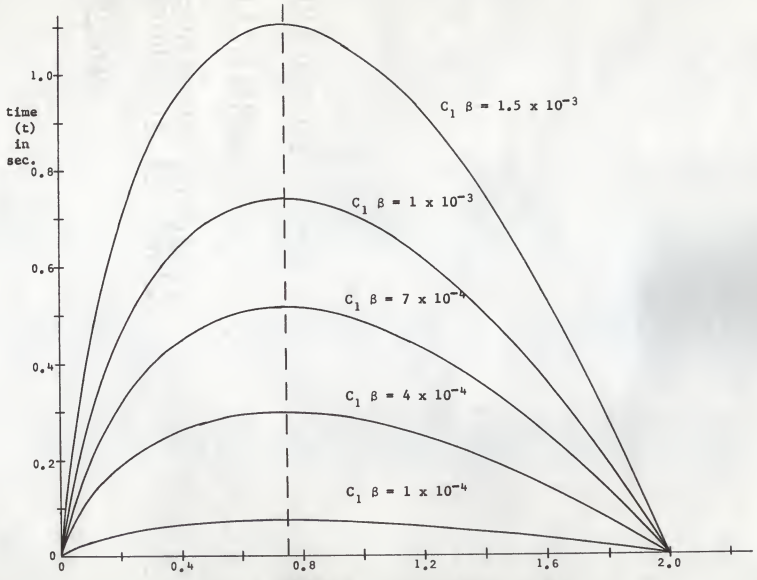


Fig. 10 Switch "ON" time versus load resistor ($R_2$).

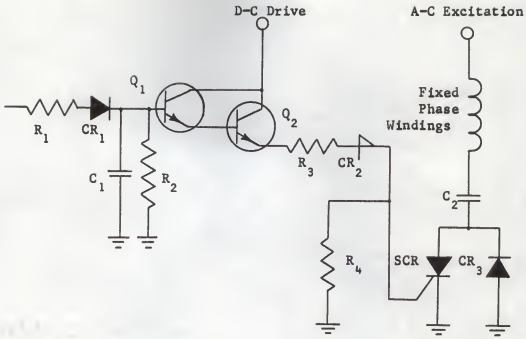


Fig. 11 Revised Shockley diode switching circuit

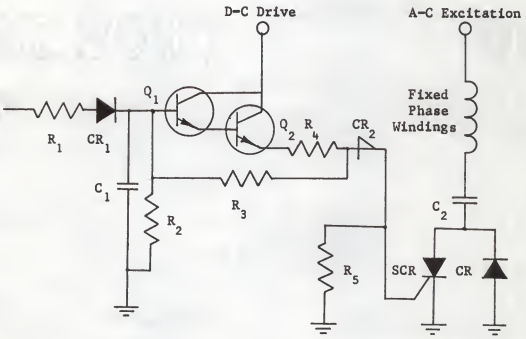


Fig. 12 Complete circuit with proper time constants

$$\beta_1 \beta_2 R_3 << R_2 \qquad (24)$$

the approximate time constant of the circuit will be

$$t = C_1 R_2 \qquad (25)$$

$R_2$ might provide too much drain on $C_1$ before the Shockley diode closes when in actual operation. An alternate circuit to provide the proper capacitor drain and also the proper time constant for the circuit is shown in Fig. 12. The time constant of the input circuit before the Shockley diode closes is given by Eq. 25. When the diode closes the time constant of the circuit is

$$t = \frac{R_2 R_3}{R_2 + R_3} C_1 \qquad (26)$$

These circuits have several advantages over the previous circuit. The advantages are:

1. Fewer components are necessary.
2. No power is required when the switch if "OFF".
3. The time constant of the circuit is easily adjusted.

## Servo System Using Fixed Phase Switch

The fixed phase switch can be incorporated in existing servo systems by making only minor changes in circuitry. As shown in Fig. 13, the fixed phases of both generator and motor are routed to the fixed phase switch instead of to ground. The stability of the system is identical to that of the system before the installation of the fixed phase switch.

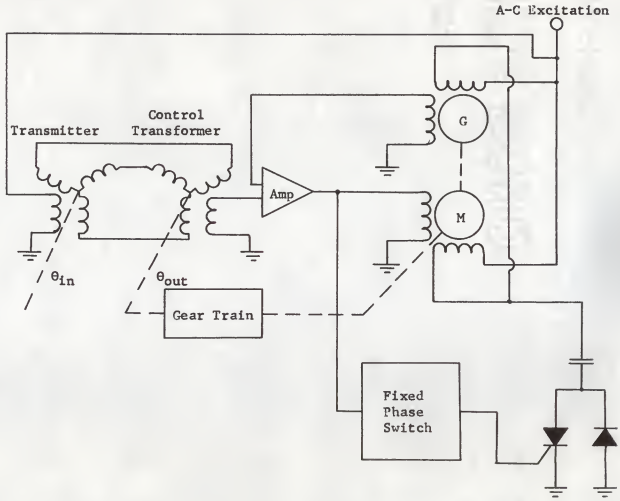


Fig. 13 Servo system configuration using fixed phase switch

The reason that the stability of both systems is the same is that before the fixed phase switch can turn "OFF", the output of the amplifier must be less than drop out voltage, i.e., near zero, for a set length of time. The analysis of a servo system used in previous instruments which will be included in the following work will give insight into the necessity of considering the non-linearities of specific system elements. The analysis of System No. 1 in terms of stability will be applicable to the system described utilizing a fixed phase switch.

There will be some difference between the system with and without the fixed phase switch in terms of threshold error necessary to produce a movement of the output. The system with a fixed phase switch can never produce a movement of the output with a smaller error than the same system without the switch. This is because a certain minimum error is necessary before the switch can be turned "ON". Less than this amount of error could cause movement of the output if the switch were not incorporated. Thus some sacrifice of system accuracy is the price that must be paid to obtain a low power servo in this manner. It should be noted, however, that once the switch is actuated, both systems will reposition with the same accuracy.

## AMPLIFIER DEVELOPMENT

The use of the fixed phase switch in connection with servomechanism operation in aircraft systems actually does not turn out to be the best approach. The basic reason for this is that while the aircraft is in flight there are constant changes in its attitude. The small changes in

attitude are large enough to actuate the switch. The system will seek its new null and after the set time the fixed phase will turn "OFF". The aircraft's attitude will again change and the process will start over again. One should keep in mind that the fixed phase is under full excitation during the new positionings of the servo. The undesirable situation can be remedied by providing a partial constant excitation to the fixed phase. This solution, however, requires heat dissipating components. The use of the fixed phase switch would work quite well in applications where accurate positioning did not occur so frequently. The possibility of developing both an amplifier and fixed phase control (not necessarily a switch) to do the required task was now considered the only feasible solution.

Certain characteristics of a readily available standard amplifier were found to be desirable and some of them were incorporated in the newly developed amplifier. The 3000 ohm input impedance of the standard amplifier was incorporated in the new amplifier to avoid other equipment changes. This made the nominal input impedance high enough so that synchro and rate generator outputs would not be drastically loaded. The transformer drive of the output stage of the standard amplifier was not desired in the new amplifier. In designing a new amplifier, several design criteria were to be met. By lowering the output impedance of the new amplifier, the servo motor could be driven with the dual control phase windings in parallel. This increased the gain of the amplifier-motor combination; however, the following requirements were still necessary.

1. The voltage gain was to be approximately 125.
2. Power output was to be 3 watts (output saturation at 13 volts).
3. Some method of controlling the fixed phase of the servo motor incorporated.

The basic amplifier which was developed using the requirements indicated has had very few circuit changes since it was originally designed. The basic circuit configuration is shown in Fig. 14. The gain of the amplifier is stabilized by both a-c and d-c feedback. The motor is driven by shifting the current in the control phase of the motor by 90°. This is accomplished by making $|X_c| = 2|X_L|$ where $X_c$ and $X_L$ are the impedance of the amplifier output capacitor and the reactive component of the motor control phase winding respectively. The output capacitor of the amplifier then serves two purposes. It provides d-c isolation to the motor windings and tunes with the motor impedance to give proper drive currents. The requirement that C of Fig. 4 must be large should now be apparent. $|X_c|$ must be small in comparison with the impedance of the fixed phase windings in Fig. 4 to provide proper phasing of the drive currents.

The fixed phase control circuit was then designed to be coupled to the amplifier and result in a torque versus input voltage characteristic of an approximate square law until the fixed phase is completely "ON". The amplifier not yet being saturated will continue to increase output torque as the input voltage is increased. Saturation of the amplifier will result at about 13 volts. The stall torque versus input voltage of the amplifier-motor combination is shown in Fig. 15.

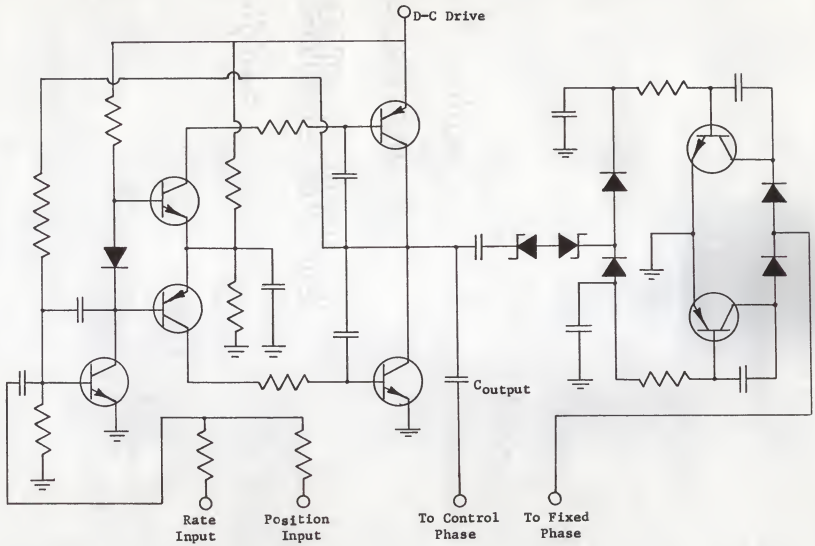


Fig. 14 High gain servo amplifier with fixed phase control

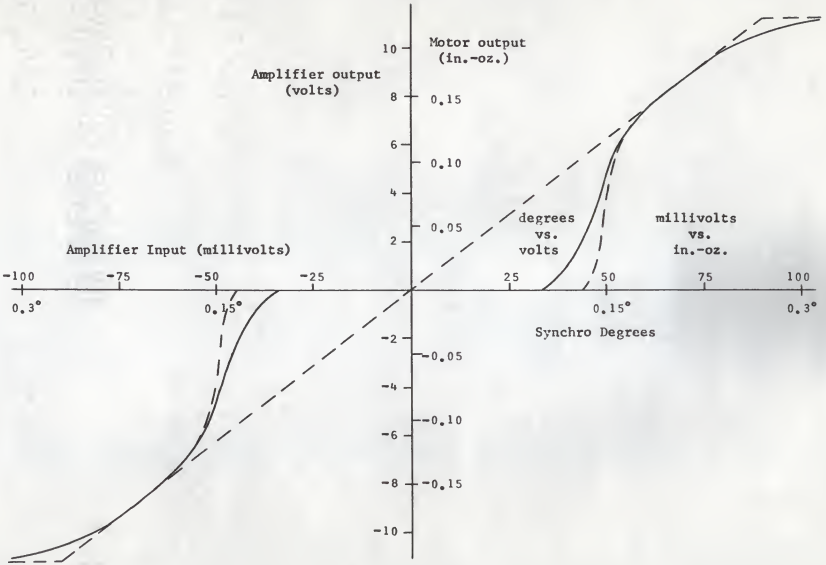


Fig. 15 Amplifier-motor gain and system amplifier gain

## OTHER ELEMENTS OF THE SYSTEM

### The Servo Motor

The servo motor used in the described system is a two-phase, 6 pole, 400-cps, size 8 motor. The fixed phase excitation should be 26 volts a-c. The fixed phase power is 3 watts maximum. The control phase of the motor has identical electrical specifications as the fixed phase when used in the series connection. The control phase consists of two windings which may be used in series or parallel. The result of the series connection is that both phases of the motor are then identical. The motor moment of inertia (including generator) is 0.65 gm-cm and the internal damping is 25 dyne-cm/rad/sec.

The speed-torque curves of the motor are shown in Fig. 16.

### The Rate Generator

The rate generator is unlike the motor in that the windings are different in characteristics. The fixed phase of the rate generator should be excited with 26 volts a-c and will consume a maximum power of 2 watts. The voltage output of the output phase is 0.325 volt/1000 rpm.

### The Error Detector

The error detector of the system is a synchro control transformer which is driven electrically by a synchro transmitter. The shaft of the control transformer is driven by the servo motor through the gear train. The electrical output of the synchro is 400 mv/deg rotation of the shaft.

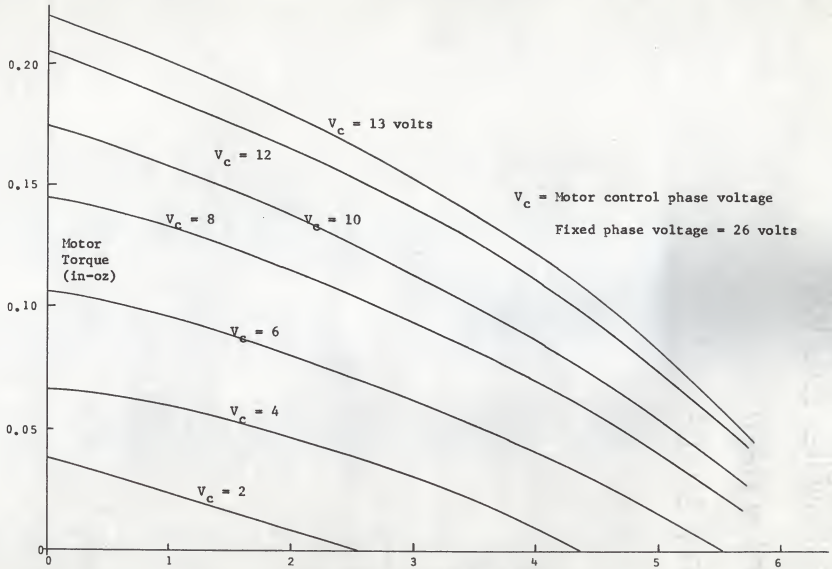


Fig. 16 Speed-torque characteristics of the servo motor

### The Gear Train

Standard gear trains used in existing instruments have ratios from 100 to 600 depending upon the particular application. Most applications, however, use ratios of approximately 360 which will be used in this study because it represents a useable value in actual system hardware and is easy to handle in calculations.

### The System Load

The load presented to the motor as reflected through the gear train is very near that of Coulomb friction. The gear train is of sufficient ratio to negate any load inertia reflected to the motor. The magnitude of the reflected Coulomb friction is, however, approximately 0.05 in-oz. The system load will effect the maximum error necessary to produce movement of the output but as will be discussed below, the load will not be used for stability analysis.

## LINEARIZING THE MOTOR CHARACTERISTICS

The normal operation of instrument servos in the system application is such that the servo motor seldom operates at high speeds. Because the movement is normally slow, the maximum torque required is also usually low. By limiting the area of interest to that indicated by the dotted rectangle in Fig. 17 a linear approximation to the motor characteristics at rated voltage on the fixed phase can be accomplished. The straight lines shown in Fig. 17 are close approximations to the speed-torque

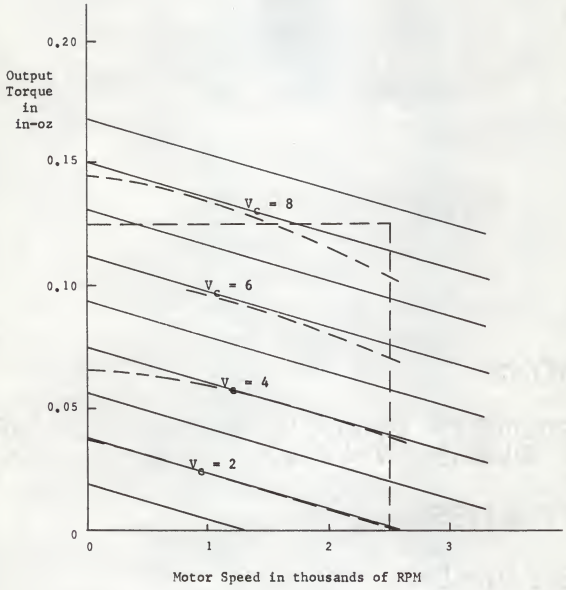


Fig. 17 Linearized speed-torque characteristics of the servo motor

curves of the motor. The following equations presented by Kuo (3) were then used to derive a transfer function for the motor.

Let

$$K_m = \frac{\text{Motor Torque (stalled)}}{\text{Control Voltage}} = \frac{0.243 \text{ in-oz}}{13 \text{ volts}} \tag{27}$$

and

$$M = -\frac{\text{Motor Torque (stalled)}}{\text{No load speed (rpm)}} = -\frac{0.075 \text{ in-oz}}{6350 \text{ rpm}} \tag{28}$$

Then

$$T_m(t) = K_m V_m(t) + M \frac{d\theta_m}{dt} \tag{29}$$

Now taking into the motor-generator mechanical characteristics gives

$$T_m(t) = K_m V_m(t) + M \frac{d\theta_m}{dt} = J_m \frac{d\theta_m^2}{dt^2} + f_m \frac{d\theta_m}{dt} \tag{30}$$

Taking transforms results in

$$K_m V_m(s) + M s \theta_m(s) = J_m s^2 \theta_m(s) + f_m s \theta_m(s) \tag{31}$$

which yields the transfer function

$$\frac{\theta_m(s)}{V_m(s)} = \frac{K_m / J_m}{s\left(\frac{f_m - M}{J_m} + s\right)} \tag{32}$$

## DETERMINATION OF SYSTEM CONSTANTS

There are a number of system constants which must be determined before a quantitative analysis can be started. The essential constants of the system are tachometer gain, position error gain, motor gain, motor

moment of inertia, motor friction, slope of the speed-torque curve, and gear ratio. The values of these constants are:

$K_T = 28.7 \times 10^{-4}$ volts/rad/sec

$K_{ct} = 20$ volts/rad

$K_m = 0.0187$ in-oz/volt

$M = -1.13 \times 10^{-4}$ in-oz-sec/rad

$f_m = 1.12 \times 10^{-4}$ in-oz-sec/rad

$J_m = 0.922 \times 10^{-5}$ in-oz-sec$^2$

$n = 360$

The value of amplifier gain is also a system constant; however, the systems analyzed will utilize different amplifier gain constants and the value used for each system will be stated in the analysis.

## AMPLIFIER CHARACTERISTICS

The input voltage versus stall torque of the amplifier-motor combination are shown in Fig. 15 by the dotted curve. This curve must be modified somewhat before applying the system error in degrees to the input scale. This must be done because some noise consisting of quadrature and higher harmonics is always present at synchro null. The fixed phase control will react to the noise voltage to turn the fixed phase "ON" even though no torque results at the motor shaft. Because the fixed phase will turn "ON" with noise voltage as well as signal voltage, the curve must be modified to that of the solid line in Fig. 15 when the input of synchro degrees is used. It is the solid curve of Fig. 15 that will be used in the analysis of systems using this amplifier.

## Describing Function of the Amplifier

In analyzing the system it will be assumed that the motor has been linearized according to Eq. 32. The amplifier transfer function will then be taken to be the same shape as the motor stall torque versus input synchro error curve. By using the curve shown in Fig. 18 as the equation of the amplifier transfer function, the system can be analyzed using describing function techniques. The describing function of the particular transfer function indicated is calculated to be as shown in Fig. 19. Note that the describing function is a function of magnitude of the input waveform only. The phase shift of the describing function is zero. This will simplify the analysis to some extent.

The actual equations of the describing function for the curve of Fig. 18 are:

$$b_1 = 0 \qquad \text{for } 0 \leq E_i \leq a$$

$$b_1 = -2k_1 a + \frac{4k_1 R}{3\pi}\sqrt{1 - (a^2/R^2)}\left(\frac{a^2}{R^2} + 2\right) + \frac{4k_1 a}{\pi}\sin^{-1}(a/R)$$

$$\text{for } a \leq E_i \leq b$$

$$b_1 = (4/\pi)\left[-\frac{k_1\sqrt{R^2 - b^2}}{3}\left(\frac{b^2}{R^2} + 2\right) + \frac{k_1\sqrt{R^2 - a^2}}{3}\left(\frac{a^2}{R^2} + 2\right)\right.$$

$$+ k_1 a \sin^{-1}(a/R) - k_1 a \sin^{-1}(b/R) + \frac{k_1 ab\sqrt{R^2 - b^2}}{R^2}$$

$$\left. - \frac{k_1 a\sqrt{R^2 - b^2}}{R^2} + k_2(\pi/4) - k_2(1/2)\sin^{-1}(b/R) + \frac{k_2 b\sqrt{R^2 - b^2}}{2R^2}\right]$$

$$\text{for } b \leq E_i \leq c$$

$$b_1 = (4/\pi)\,\frac{k_1}{3}\left\{\sqrt{R^2 - a^2}\left(\frac{a^2}{R^2} + 2\right) - \sqrt{R^2 - b^2}\left(\frac{b^2}{R^2} + 2\right)\right\}$$

$$+ k_1 a\left(\sin^{-1}(a/R) - \sin^{-1}(b/R) + \frac{b\sqrt{R^2 - b^2} - a\sqrt{R^2 - b^2}}{R^2}\right)$$

$$+ \frac{k_2}{2}\left(\sin^{-1}(c/R) - \sin^{-1}(b/R)\right) + \frac{k_2}{2R^2}\left(b\sqrt{R^2 - b^2} - c\sqrt{R^2 - c^2}\right)$$

$$+ \frac{V_{max}}{R^2}\sqrt{R^2 - c^2} \qquad \text{for } c < R \qquad (33)$$

where $E_i = R \sin(\omega t)$, $k_2 = (V_{max}/c)$, and $k_1 = k_2 \dfrac{b}{(b - a)^2}$

## SYSTEM ANALYSIS

The performance in terms of stability will be presented for four systems. There are other characteristics of instrument servomechanisms that are quite important such as threshold and maximum speed of response. These characteristics will not be analyzed for they can usually be determined quite easily. The threshold can be decreased by increasing the gain of the amplifier and the speed of response is usually set by a simple calculation. This calculation assumes that the maximum motor speed in the system is 60 to 75 percent of the maximum rated motor speed. This in turn determines the length of the gear train from motor to load. Servo systems in instruments must be stable; therefore stability will be the main concern in this analysis.

The first system to be analyzed will be an ideal servo system. By presenting the basic stability principles for the ideal system, insight

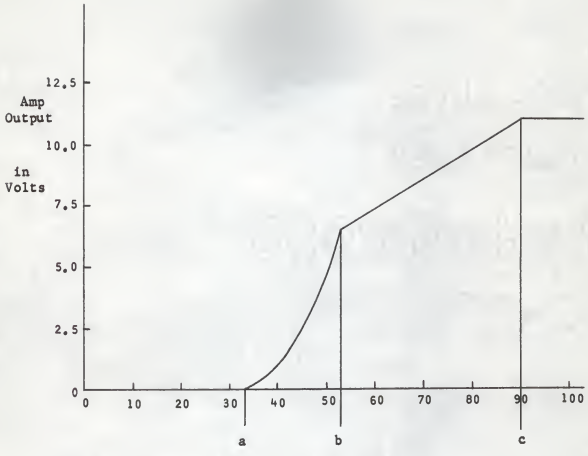


$$V_o = 0 \ , \ 0 \leq E_i \leq a$$

$$V_o = k_1(E_i - a)^2, \quad a \leq E_i \leq b \qquad k_2 = \frac{V_{max}}{c}$$

$$V_o = k_2 E_i \quad , \quad b \leq E_i \leq c \qquad k_1 = k_2 \frac{b}{(b - a)^2}$$

$$V_o = V_{max} = c\, k_2 \ , \ c \leq E_i$$

Fig. 18 Simplified amplifier characteristics

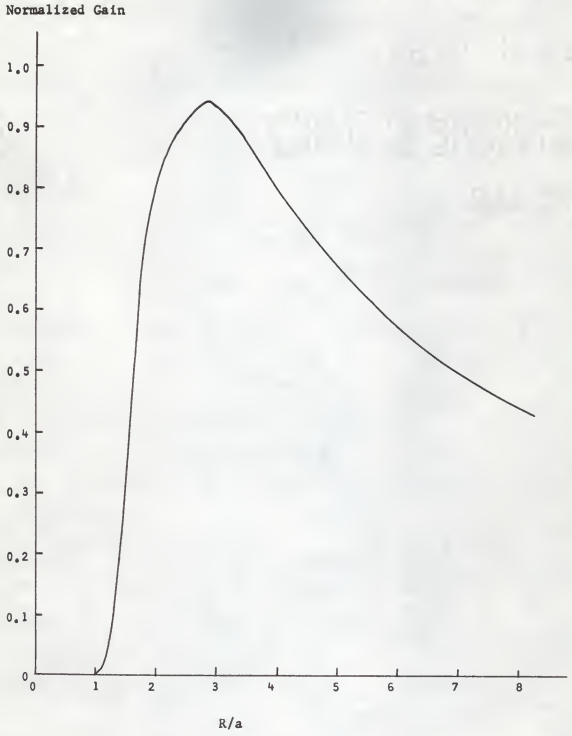


Fig. 19 Amplifier describing function gain characteristics

can be gained with regard to the analysis of more complex systems which involve non-linearities. In fact, the analysis of the first system coupled with laboratory observations of system performance will point out the necessity to analyze certain non-linearities of the systems that follow.

System No. 1

The basic block diagram of this system is shown in Fig. 20. One method of arranging the system to give a unity feedback configuration is to combine the dotted block into a simple transfer function and reduce the system to that of Fig. 21. The root locus of the system which is shown in Fig. 21 is then plotted as shown in Fig. 22. This plot is, of course, for a fixed value of $AK_mK_T$. Notice, however, that A is the amplifier gain which is the parameter varied to obtain the root locus plot. Therefore in actuality the pole labled $-(f_m - M + AK_mK_T)/J_m$ moves left as the value of A is increased. In fact, for this system the pole moves left faster than the increase in gain moves the root locus right and the amplifier gain may be increased indefinitely and still maintain stability.

A more realistic way to arrange the system elements for the root locus technique of analysis is to combine the blocks as shown in Fig. 23. Further manipulation results in the system shown in Fig. 24. The output of the system will be stable only if the loop is stable. By examining only the loop, it can easily be seen that the open loop gain is given by the equation

$$G = \frac{\{(A\ K_m\ K_T)/J_m\}(s + \{K_{ct}/nK_T\})}{s\{s + (f_m - M)/J_m\}} \qquad (34)$$

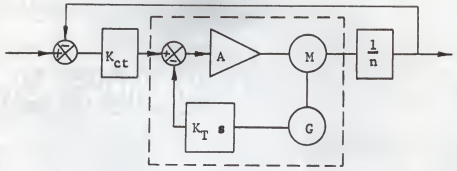


Fig. 20 Block diagram of System No. 1

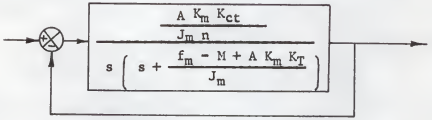


Fig. 21 System No. 1 in unity feedback configuration

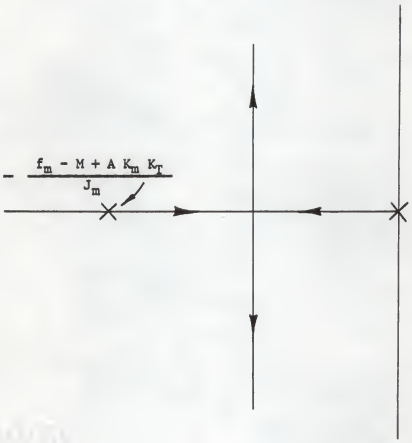


Fig. 22 Root locus of System No. 1 in unity feedback configuration

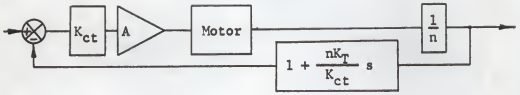


Fig. 23 System arrangement with single feedback loop

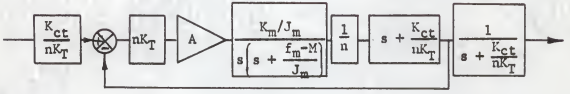


Fig. 24 System arrangement to have unity feedback

Using the standard root locus technique, the poles and zero of the open loop transfer function are plotted. This system fits into a recognizable root locus pattern shown in Fig. 25. Observation of the root locus plot indicates that as the rate feedback is reduced to zero, the zero moves left to $-\infty$. For the value of rate feedback gain ($K_T$) used the root locus will never leave the negative real axis. If the rate feedback gain ($K_T$) were one half of its indicated value, then the zero would be outside the two poles and the form of the root locus would be like that of Fig. 26.

System No. 2

Review of the analysis results for System No. 1 indicates that the system will never be unstable. The analysis indicates that with no rate feedback the system is highly underdamped but yet stable. This theory seems to be in direct contradiction with observed laboratory results when the rate feedback of the system has been lost. Oscillations can be established and maintained in all equipments using the described system when rate feedback is absent. The only possible cause of oscillations seems to lie in the gear train. By assuming a small amount of backlash in the gear train, System No. 2 is established as shown in Fig. 27.

Backlash has been analyzed by many authors using describing function techniques. As shown by Savant (6), the backlash describing function is given by the magnitude of the fundamental component of the output when a sine wave function is applied at the input. The phase angle of the describing function is the amount of phase shift between the fundamental

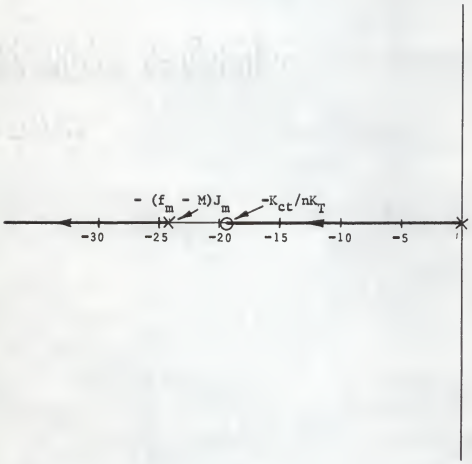


Fig. 25 Root locus plot of System No. 2

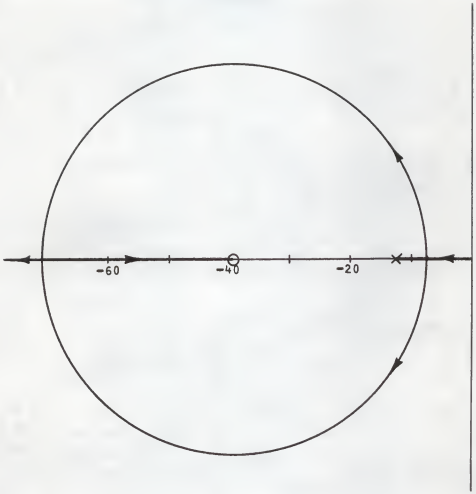


Fig. 26 Root locus of System No. 2 with one half normal rate gain.

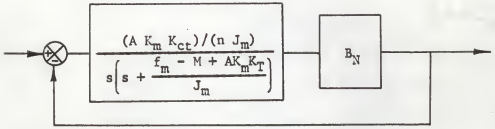


Fig. 27 Feedback system showing linear and non-linear portions

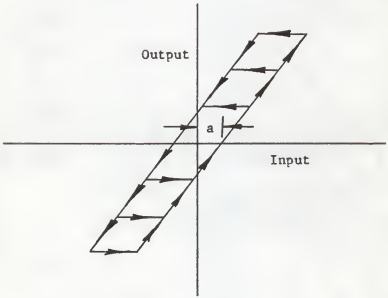


Fig. 28 Transfer characteristics of gear train backlash

component of the output and the input. Calculations reveal the describing function of the backlash characteristic as shown in Fig. 28 to be

$$B_{N_1} = \sqrt{a_1^2 + b_1^2}$$
$$\Phi_{N_1} = \tan^{-1}(a_1/b_1) \tag{35}$$

where

$$a_1/A = (a/\pi A)(\{a/A\} - 2)$$
$$b_1/A = (1/\pi)(\{\pi/2\} + \omega t_1 + (1 - \{a/A\})\cos\{\omega t_1\}) \tag{36}$$

These equations are for an input of A sin(ωt). The amplitude and phase plots of the backlash non-linearity are shown in Fig. 21. The negative reciprocal of the backlash characteristic is plotted in Fig. 30 and Fig. 31. Upon taking into account the backlash of the gear train, another system is established to analyze for stability. The system then consists of the linear and non-linear portions as shown in Fig. 27. The transfer function is

$$\frac{\Theta_o}{\Theta_i} = \frac{G\, B_N}{1 + G\, B_N} \tag{37}$$

where G is the linear portion of the system.

The stability of the system is analyzed by examining the characteristic equation $1 + G\, B_N = 0$. This is done by plotting G and $-(1/B_N)$ on a Nichols chart and/or Nyquist plot. If the plots of G and $-(1/B_N)$ ever have a common point, then the possibility of oscillations is present. The functions $-(1/B_N)$ and G are plotted in Fig. 30 and Fig. 31. Two plots

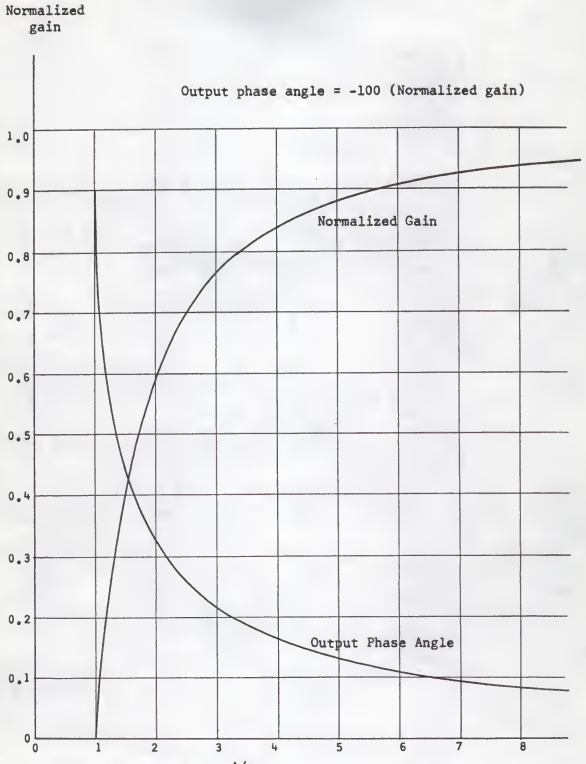


Fig. 29 Gain-phase characteristics of the backlash non-linearity

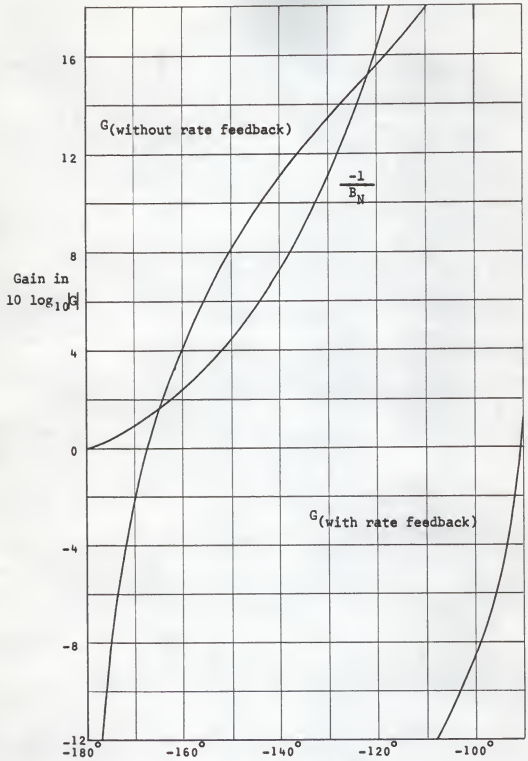


Fig. 30 Nichols chart of System No. 2

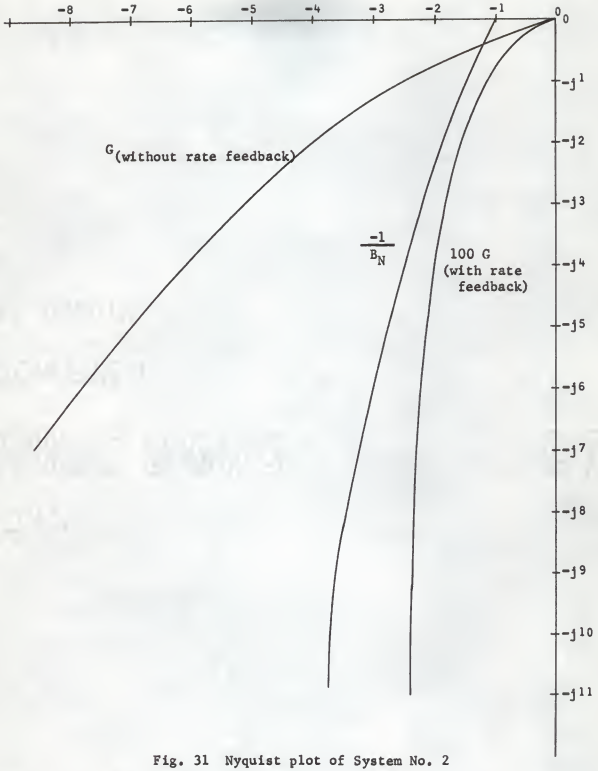


Fig. 31 Nyquist plot of System No. 2

of G are shown; one for the system with rate feedback and one for the system with no rate feedback. The plots clearly indicate that oscillations are possible with no rate feedback. Note should be taken of the fact that the function 100G is plotted on the Nyquist plot for the condition with no rate feedback instead of G to make the scales more compatable.

System No. 3

The analysis of systems thus far presented has assumed a linear amplifier in conjunction with both linear and non-linear system elements. It was shown that the non-linearity of the backlash in the gear train can cause oscillations in a system with no rate feedback. Adding another non-linearity, namely that of the non-linear amplifier, whose characteristics are shown in Fig. 15, results in System No. 3. The resulting system contains two non-linear elements and such a system is very difficult to analyze analytically.

An attempt was made, however, to make an analytic analysis of the system with two non-linearities by maximizing the function $G|\underline{-135°}$. This was done by substituting $j(f_m - M + AK_mK_T)/(J_m)$ for s and then setting $(\partial|G|)/(\partial A) = 0$ which yielded A = 4.2.

This value of A in G given by Eq. 34 should give a Nyquist plot nearly as close to the plot of $-(1/B_N)$ as G can get with any gain A. Figure 32 shows the plot of 10G when A = 4.2. The two plots do not have a common point; therefore System No. 3 with two non-linearities should always be stable. The analytic analysis of System No. 3 appeared to be non-conclusive. For this reason the analog computer was used to simulate the system

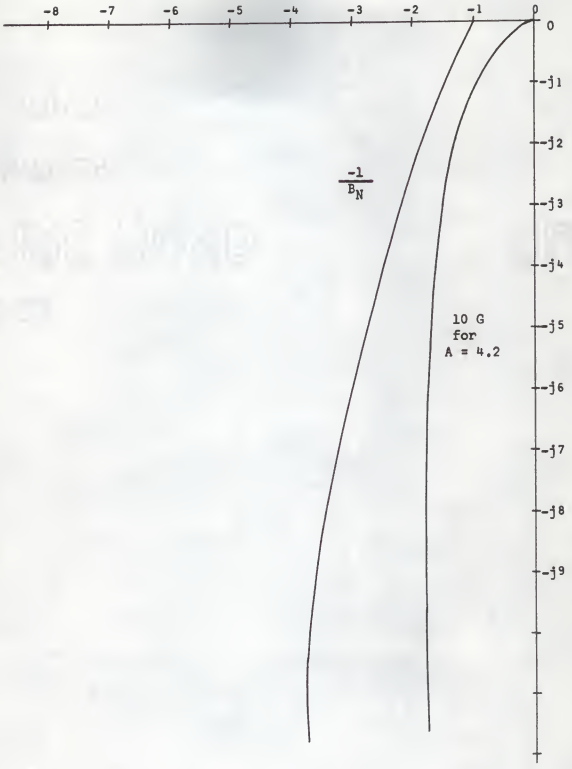


Fig. 32 Nyquist plot of System No. 3

and an extension of it (System No. 4).

In System No. 1 and System No. 2 the load was assumed to be very small. This is indeed the case in most instruments where these servos are used. As mentioned above, the system load for System No. 3 and System No. 4 is a significant portion of the maximum motor output torque. The reason the system load was not considered in the servo simulation of the last two systems is that the load being almost entirely Coulomb friction has a stabilizing effect on the system. In actual practice, however, backlash exists between the feedback device (synchro) and the load. This is in addition to the backlash that exists between the motor output shaft and the synchro. It is therefore entirely possible for oscillations to exist in the feedback loop and yet not move the load. The load was therefore not considered in the simulation.

### System No. 4

This system is very similar to System No. 3. The difference lies in the drive of the rate generator fixed phase winding. System No. 3 assumed a constant drive to the fixed phase of the rate generator while System No. 4 uses the fixed phase control of the amplifier to drive the fixed phase of the rate generator as well as the fixed phase of the motor. The difference between the simulation of the two systems can be seen in Fig. 36.

## SIMULATION AND RESULTS

The simulation of the two systems required that three non-linearities be used. These were the amplifier, backlash, and rate generator feedback

drive. These three non-linearities were then combined with conventional analog computer techniques to simulate the desired systems.

## Amplifier Simulation

The actual amplifier shows a square-law characteristic until the fixed phase control is completely "ON." As the input increases further, the output increases linearly with input and finally saturates. The actual amplifier was simulated by using a series of straight lines to approximate the curve. Figure 33 shows curves of the actual amplifier output (similar to Fig. 15) and the simulation used. Only the positive portion of the transfer characteristic is shown; however the simulation was symmetric. The simulation was accomplished by using a limiter for the saturation characteristic, followed by three dead-band diode circuits. The dead-band output gains were controlled with potentiometers of the computer. The schematic of the amplifier simulation is shown in Fig. 34.

## Backlash Simulation

The backlash characteristic was simulated with standard techniques. The backlash simulation is shown in Fig. 35.

## Rate Generator Drive Excitation

The rate generator feedback voltage of System No. 4 is a function of the amplifier output voltage and the speed of the motor. The simulation of the exact characteristic was done with a servo multiplier. The simulation schematic of System No. 3 and System No. 4 is shown in Fig. 36.

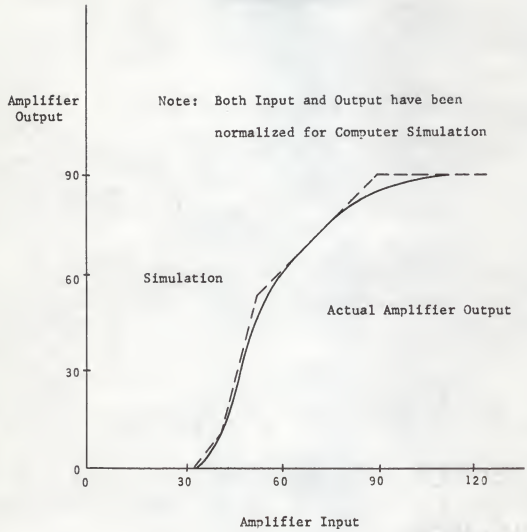


Fig. 33 Analog computer simulation curve for servo amplifier

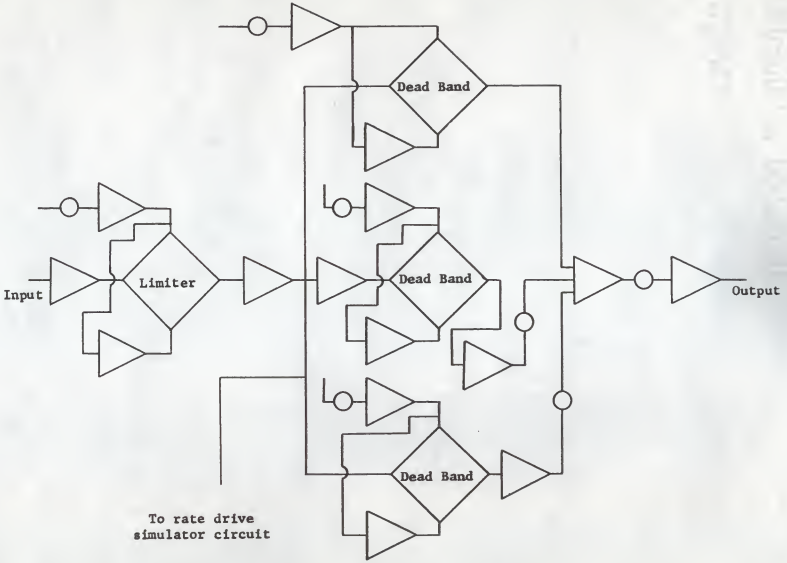


Fig. 34 Analog computer simulation of the servo amplifier

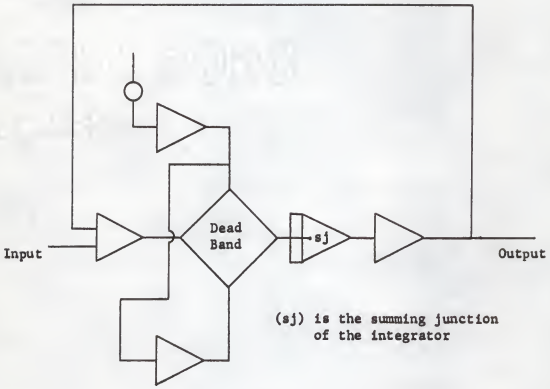


Fig. 35 Analog computer simulation of backlash

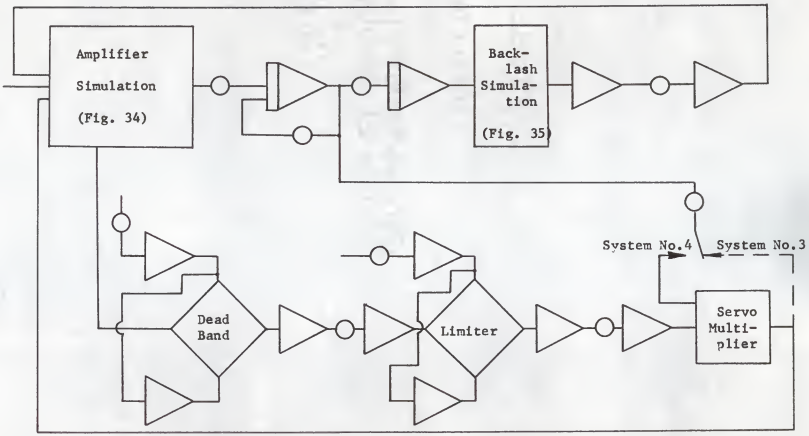


Fig. 36 Analog symulation of System No. 3 and System No. 4

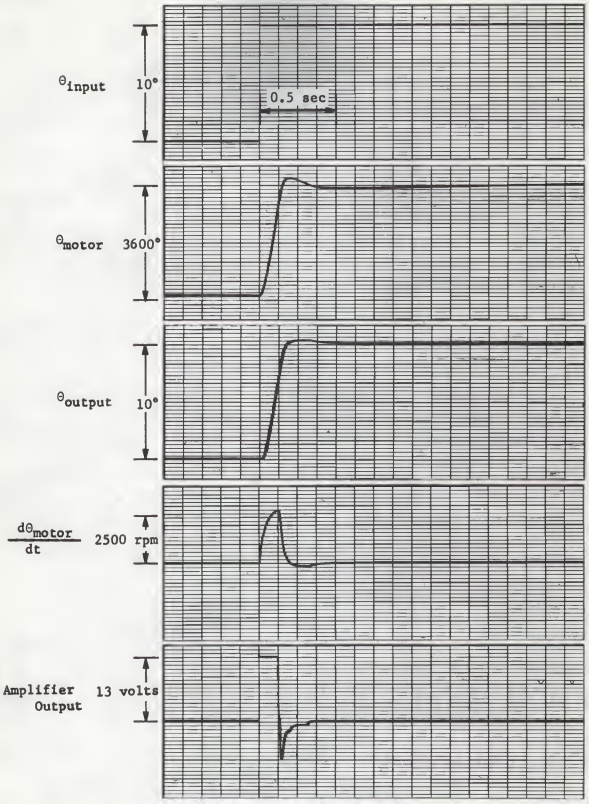


Fig. 37 Response of System No. 3 to a step input

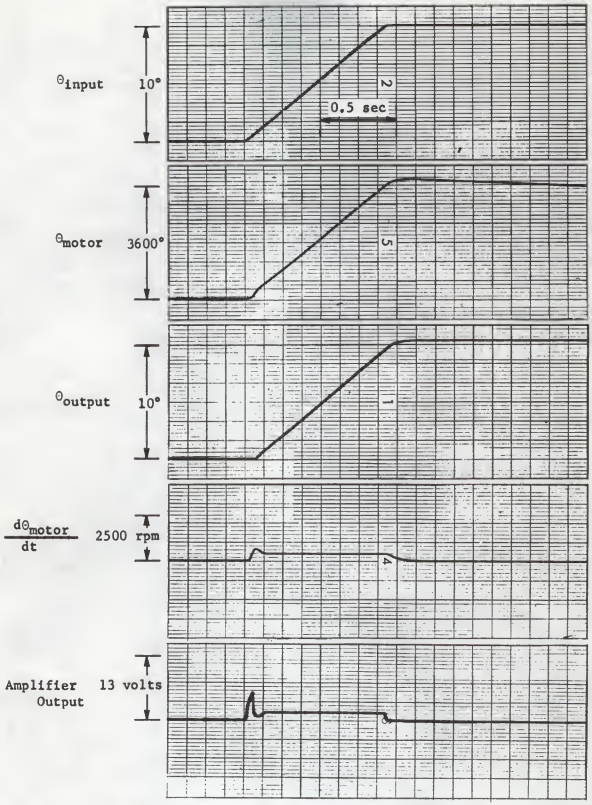


Fig. 38 Response of System No. 3 to a ramp input

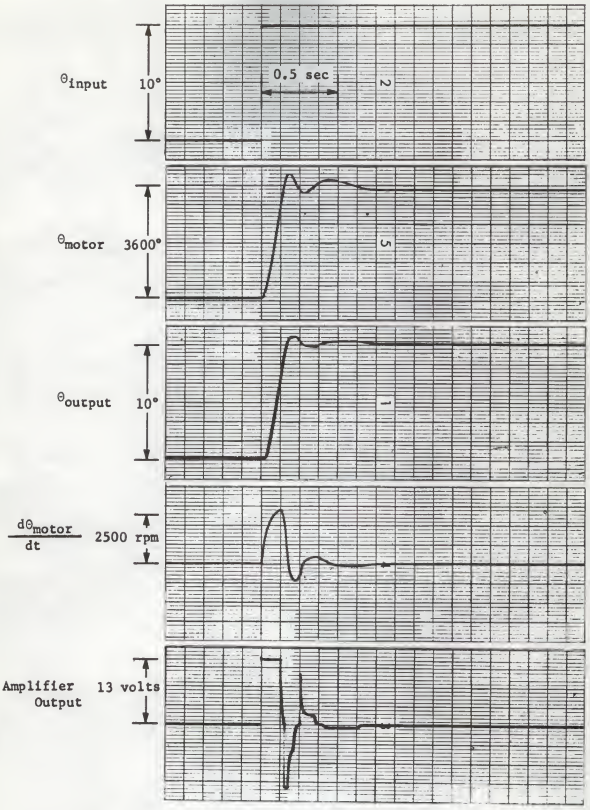


Fig. 39 Response of System No. 4 to a step input

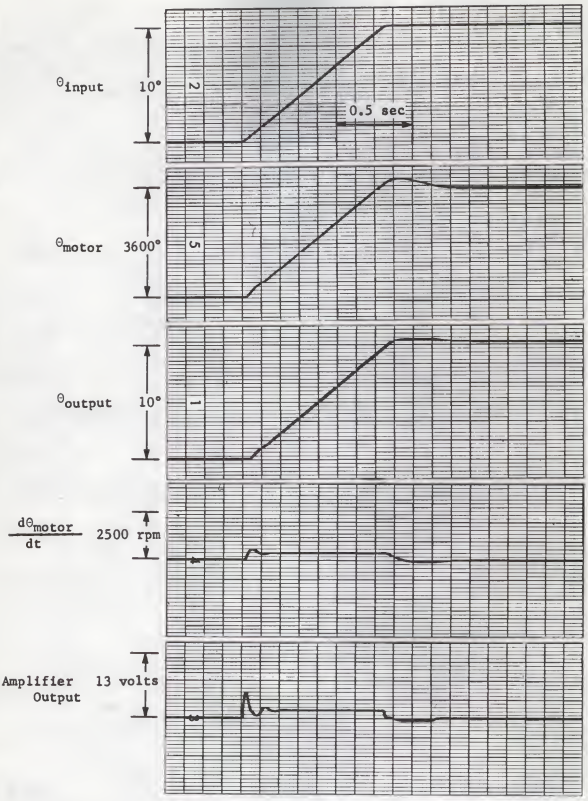


Fig. 40 Response of System No. 4 to a ramp input

## Results

The results of the simulation are presented in Figs. 37 through 40. Figures 37 and 38 are for System No. 3 and Figs. 39 and 40 are for System No. 4. Data is presented for the system response to a step input and to a ramp input. The step inputs are approximately 10 degrees in magnitude. The simulation was slowed down by a factor of 100 to 1 and the time scale of the data is 25 seconds per centimeter. Converting to the actual system response would give 0.25 second per centimeter. The data of Fig. 37 shows that System No. 3 will position 10 degrees in approximately 0.15 second.

The data does show that both systems are stable. Note in each case that the power to the motor is much less than would be consumed had the fixed phase control not been used. Actual flight data has been obtained for System No. 3 which shows that the power to the fixed phase of the motor has been reduced from 3 watts to 0.161 watt. The fixed phase power of the generator during these flight tests was 2 watts.

## CONCLUSIONS

On the basis of the simulation data presented, it would seen reasonable to recommend that a system using rate feedback control (System No. 4) be incorporated. Although there is some loss in system damping by using the fixed phase control for the rate generator, the system does position with very few overshoots. A system with overshoots is not necessarily unacceptable for use in aircraft instruments. The rate generator fixed phase control could be incorporated with no additional circuitry which makes the scheme even more attractive for present use.

Further study in the area of fixed phase control would be advantageous. Motor damping as a function of amplifier output is one area which, if taken into account, could change the simulator output results. It might also be possible to obtain a more optimum balance of rate feedback and position feedback. The positioning accuracy of System No. 4 will be equal to that of System No. 3 since the same motor power is available to position the load. Essentially both systems have almost the same performance; the difference being that System No. 4 has somewhat less damping than System No. 3.

It is therefore recommended that the rate generator fixed phase be controlled in the same manner as the fixed phase of the motor. Power reduction of approximately 20 to 1 can be accomplished in going from a system such as System No. 2 to System No.4. This increases the operating efficiency of the system and accomplishes the original purpose of reducing the operating temperature of the instruments in which these servomechanisms are used.

ACKNOWLEDGMENTS

The author expresses appreciation to Dr. Charles H. Murrish, his major advisor, for encouragement, helpful suggestions, and guidance in preparing this thesis. Acknowledgment is also due to Collins Radio Company at Cedar Rapids, Iowa where the author was employed and actively involved in projects pertaining to the thesis topic. The author also expresses appreciation to many of his colleagues at Collins Radio Company who offered suggestions and gave constant encouragement in preparing this thesis.

REFERENCES

(1) Ahrendt, William R. and Savant, Clement J. Jr.
Servomechanism Practice. New York: McGraw-Hill, 1960.

(2) Gibson, John E. and Tuteur, Franz B.
Control System Components. New York: McGraw-Hill, 1958.

(3) Kuo, Benjamin C.
Analysis and Synthesis of Sample Data Control Systems. Englewood Cliffs, N. J.: Prentice-Hall, 1963.

(4) Levison, Emanuel
Non-Linear Feedback Control Systems. Reprinted from the magazine Electro-Technology. New York: C-M Technical Publications Corporation, 1962.

(5) Rogers, A. E. and Connolly, T. W.
Analog Computation in Engineering Design. New York: McGraw-Hill, 1960.

(6) Savant, Clement J. Jr.
Basic Feedback Control System Design. New York: McGraw-Hill, 1958.

(7) Thaler, George J. and Pastel, Marvin P.
Analysis and Design of Nonlinear Feedback Control Systems. New York: McGraw-Hill, 1962.

(8) Thaler, George J.
Servomechanism Theory. New York: McGraw-Hill, 1955.

(9) Thaler, George J. and Brown, Robert G.
Analysis and Design of Feedback Control Systems. New York: McGraw-Hill, 1960.

(10) Truxal, John G.
Control System Synthesis. New York: McGraw-Hill, 1958.

# DEVELOPMENT AND ANALYSIS OF A LOW POWER A-C INSTRUMENT SERVOMECHANISM

by

JOHN IRVIN GARRETT

B. S. Kansas State University, 1960

---

AN ABSTRACT OF A MASTER'S THESIS

submitted in partial fulfillment of the

requirements for the degree

MASTER OF SCIENCE

Department of Electrical Engineering

KANSAS STATE UNIVERSITY
Manhattan, Kansas

1964

This thesis describes the elements and operation of servomechanisms used in modern aircraft flight instruments. The problem area which is developed and analyzed is that of heat reduction in the two phase, 400 cycle per second servo motors. This problem was created when additional display functions were desired in the flight instrument.

The first section of the thesis presents development and analysis of circuits used to switch the fixed phase of the a-c servo motors. Heat reduction is accomplished by turning the fixed phase of the motors "OFF" at null. Some very interesting timing relations are generated by the fixed phase switch drive circuits. A better method of heat reduction can be accomplished, however, through the use of a fixed phase control rather than switch.

A system is analyzed using actual system constants and is shown to be stable even if rate feedback from the rate generator is lost. Since laboratory observations contradict this analysis, gear train backlash was included in the analysis of the systems that followed to make the mathematical model more exact.

Two systems were analyzed with the aid of the analog computer. This tool was used to properly account for the non-linearities of the systems analyzed. The first of these systems is presently being used and the second has application possibilities. This second system makes use of the fixed phase control on the rate generator as well as the motor. This system can give an overall heat reduction of 20 to 1 with only slight reduction in the system damping.